The Journal of Immunology

# A Dual Role for Talin in NK Cell Cytotoxicity: Activation of LFA-1-Mediated Cell Adhesion and Polarization of NK Cells

Emily M. Mace, Susan J. Monkley, David R. Critchley and Fumio Takei



*J Immunol* 2009; 182:948-956; ;
doi: 10.4049/jimmunol.182.2.948
http://www.jimmunol.org/content/182/2/948



*The Journal of Immunology* is published twice each month by
The American Association of Immunologists, Inc.,
1451 Rockville Pike, Suite 650, Rockville, MD 20852

Print ISSN: 0022-1767 Online ISSN: 1550-6606.

# A Dual Role for Talin in NK Cell Cytotoxicity: Activation of LFA-1-Mediated Cell Adhesion and Polarization of NK Cells[1]

**Emily M. Mace,*† Susan J. Monkley,§ David R. Critchley,§ and Fumio Takei[2]*‡**

**LFA-1 is critical for NK cell cytotoxicity because it mediates adhesion of NK cells to target cells. Talin is thought to associate with the cytoplasmic tail of LFA-1 and activates its ligand-binding function. In this study, we report that talin is also required for LFA-1-mediated outside-in signaling leading to NK cell polarization. NK cells generated from talin1-deficient murine embryonic stem cells are defective in LFA-1-mediated adhesion. Although exogenously added manganese activates LFA-1 on talin-deficient NK cells and induces conjugate formation with target cells, their LFA-1-dependent cytotoxicity is impaired. Binding of ICAM-1-coated beads to wild-type NK cells induces reorganization of the actin cytoskeleton and coligation of the activating receptor NKG2D induces polarization of cytotoxic granules, whereas talin1-deficient NK cells fail to polarize with or without NKG2D coligation. Thus, talin1 plays a dual role in NK cell cytotoxicity, first by activation of LFA-1-mediated adhesion and then via LFA-1-induced NK cell polarization.** *The Journal of Immunology,* **2009, 182: 948–956.**

Natural killer cells kill virus-infected cells and tumor cells without prior immunization. Killing of target cells by NK cells is a multistep process. The first step is the binding of NK cells to target cells, which is mediated by cell adhesion molecules. This is followed by polarization of NK cells, translocation of cytotoxic granules toward the target cells, and finally the release of perforin and granzymes contained in the cytotoxic granules toward the bound target cells. The leukocyte integrin LFA-1 ($\alpha_L\beta_2$ integrin, CD11a/CD18) plays an essential role in natural cytotoxicity of NK cells as it mediates binding of NK cells to target cells. NK cells from LFA-1-deficient mice are unable to kill target cells due to impaired conjugate formation (1). Blocking Abs to LFA-1 also inhibit NK cell cytotoxicity by inhibiting NK cell binding to target cells (2, 3). Although the importance of LFA-1 in NK cell-target cell adhesion has been well established, recent studies have suggested that LFA-1 may also play a role in signaling events initiated by binding to its primary ligand ICAM-1. In T cells, LFA-1 acts as a costimulatory molecule by lowering the threshold for TCR-mediated signals required for T cell activation. Engagement of LFA-1 in the absence of TCR signals results in the formation of an "actin cloud," in which actin-, LFA-1-, and tyrosine-phosphorylated proteins are found in a ring at the contact site between a T cell and an APC (4). In NK cells, LFA-1 has been implicated in a number of signaling processes associated with cytotoxicity. These include granule polarization (5), Vav1 phosphorylation (6), and Pyk2 phosphorylation (7). However, the mechanism by which LFA-1 transduces signals leading to these events remains unclear.

NKG2D is one of the best-characterized activating receptors on NK cells and is thought to be responsible for the killing by NK cells of tumor cells and virus-infected cells, which often express NKG2D ligands, including RAE1, MULT, and H60 in mice (8–11). In mice, NKG2D associates with both DAP10 and the ITAM-bearing DAP12 adaptors. ITAM-coupled receptor signaling in NK cells is similar to that of the B cell or TCR, as Src family kinases, Syk, and ZAP70 mediate signals that converge on downstream targets such as the MEK/ERK pathway, Akt, and NF-$\kappa$B. Although many NKG2D signaling intermediates that lead to NK cell activation have been identified, NKG2D ligation alone seems insufficient for the degranulation of NK cells and efficient cytotoxicity requires costimulatory signals (12) Thus, the exact mechanisms by which NKG2D promotes NK cell cytotoxicity still remain to be elucidated.

Talin is a large (~270-kDa) cytoskeletal adaptor protein that is a ubiquitous component of focal adhesion complexes of adherent cells (13). Talin has an N-terminal globular head with a Band 4.1 ezrin radixin moesin (FERM) domain containing a binding site for the cytoplasmic tails of integrin $\beta$-chains (14) and an actin binding site (15). It also contains binding sites for focal adhesion kinase and the type 1 $\gamma$ isoform of the phosphoinositide 4,5-kinase (16–18). The C-terminal talin rod contains a second integrin binding site (19), at least two actin binding sites (15), and multiple binding sites for vinculin, which itself binds actin (20, 21). Talin is thought to be critical for the activation of integrins. Binding of the talin FERM domain to the cytoplasmic tail of the $\beta$ integrin subunit induces separation of the tails of the two integrin chains, which results in a rapid transition to a high-affinity conformation (22, 23). Thus, overexpression of talin head activates LFA-1 (22). In resting lymphocytes, talin is mostly found in the cytosol and is thought to be in an inactive form due to a head-tail interaction. Upon cell activation, talin is thought to be released from the self-inhibited state, bind to the cytoplasmic tails of integrins, and induce their conformational changes by separating the two chains (24). Recent studies using selective deletion of talin1 in hematopoietic cells show that talin1 is required for the activation of $\beta_1$ and $\beta_3$ integrins

*Terry Fox Laboratory, British Columbia Cancer Agency, Vancouver, British Columbia, Canada; †Genetics Graduate Program and ‡Department of Pathology and Laboratory Medicine, University of British Columbia, Vancouver, British Columbia, Canada; and §Department of Biochemistry, University of Leicester, Leicester, United Kingdom

Received for publication August 19, 2008. Accepted for publication November 6, 2008.

The costs of publication of this article were defrayed in part by the payment of page charges. This article must therefore be hereby marked *advertisement* in accordance with 18 U.S.C. Section 1734 solely to indicate this fact.

[1] This work was supported by grants from the Canadian Institutes of Health Research (to F.T.) and the Wellcome Trust (to D.R.C.).

[2] Address correspondence and reprint requests to Dr. Fumio Takei, Terry Fox Laboratory, British Columbia Cancer Agency, 675 West 10th Street, Vancouver, British Columbia, V5Z 1L3, Canada. E-mail address: ftakei@bccrc.ca

in platelets. In addition, talin1 is required for $\alpha_{IIb}\beta_3$ integrin-mediated cell spreading (25). Thus, talin appears able to transduce signals resulting in integrin activation as well as those induced by integrin ligand occupancy.

In the immune synapse formed between a NK cell and a sensitive target (often termed a "cytolytic immune synapse"), LFA-1, talin, and actin form a ring that provides stability to the immune synapse and acts as the scaffold for the assembly of specialized signaling complexes (26). In addition, this ring may act as a guide for the delivery of cytotoxic granules to be delivered in a lethal hit to the target (26). The signals that cause the accumulation of actin and talin in the immune synapse with LFA-1 are not known. Polarization of the microtubule organization center (MTOC)[3] toward the target is also required for cytotoxicity, and this polarization is followed by the accumulation of cytotoxic granules at the immune synapse (26). Both the MTOC and granules are found to accumulate in the center of the LFA-1-talin-actin ring and it has been observed in CTL that microtubules are anchored in the LFA-1 ring (27).

To determine the role that talin plays in LFA-1-mediated NK cell functions, we generated talin1-knockout (KO) NK cells from *Tln1*$^{-/-}$ embryonic stem (ES) cells in vitro. Our analyses of talin1-KO NK cells suggest that talin plays a dual role. Initially, it is required for LFA-1-mediated cell adhesion, presumably by inside-out activation of LFA-1 conformation. Talin1 is then also required for outside-in signaling via ligand-bound LFA-1, resulting in the reorganization of the actin cytoskeleton and NK cell polarization, both of which are essential for NK cell cytotoxicity. Our results also clarify the role of LFA-1 in NK cell cytotoxicity. Binding of ICAM-1 to LFA-1 mediates initial binding of NK cells to target cells. It also induces reorganization of the actin cytoskeleton, but not polarization of cytotoxic granules. Although cytotoxic granule polarization can be induced by coligation of the activating receptor NKG2D, reorganization of the actin cytoskeleton mediated by LFA-1 is a talin1-dependent process and is required for granule polarization.

## Materials and Methods

### *Mice, Abs, reagents, and flow cytometry*

C57BL/6 mice were bred in the British Columbia Cancer Research Centre Animal Research Centre. All animal use was approved by the animal care committee of the University of British Columbia and animals were maintained and euthanized under humane conditions in accordance with the guidelines of the Canadian Council on Animal Care. *Tln1*$^{-/-}$ ES cells and WT ES cells have been described (28). OP9 stromal cells were from RIKEN (Tokyo, Japan). L cells and ICAM-1-transfected L cells have been previously described (29). Anti-CD44 mAb was a gift from Dr. P. Johnson (University of British Columbia, Vancouver, Canada). YAC-1 cells, the mouse anti H-2K$^k$ hybridoma (16-3-22S) and rat anti-murine LFA-1 hybridoma (TIB213) were from American Type Culture Collection. 2.4G2 (anti-FcR$\gamma$) has been previously described (30). Biotinylated anti-CD34 (RAM34) mAb was purchased from eBioscience. FITC-conjugated anti-NKG2D and PE-conjugated streptavidin were purchased from BD Biosciences. Anti-talin mAb (8D4) was from Sigma-Aldrich. Anti-ß-tubulin mAb (KMX-1) was from Chemicon International. Anti-phospho-Pyk2 (Tyr$^{402}$) mAb (RR102) and anti-phosphotyrosine (4G10) were from Upstate Biotechnology. Anti-Pyk2 (N-19) was from Santa Cruz Biotechnology. Polyclonal anti-granzyme B (ab4059) was from Abcam. Rhodamine-conjugated phalloidin, Alexa Fluor 647 phalloidin, Alexa Fluor 488-conjugated goat anti-mouse IgG, Alexa Fluor 568-conjugated donkey anti-rabbit IgG and rabbit anti-goat IgG were purchased from Invitrogen and Molecular Probes. CFSE was purchased from Invitrogen and Molecular Probes. Murine recombinant soluble ICAM-1 (sICAM-1) (31) was from StemCell Technologies. Manganese chloride solution was from MJS Biolynx. Polystyrene beads were from Polysciences. For flow cytometry, cells were first preincubated with 2.4G2 supernatant followed by primary mAbs. All incubations were performed at 4°C for at least 30 min and stained cells were subsequently analyzed on a FACSCaliber (BD Biosciences). Flow cytometry results were analyzed using WinMDI (Scripps Research Institute, La Jolla, CA). Cell sorting was conducted on a FACSVantage SE (BD Biosciences).

### *Generation of ES-derived NK cells*

Generation of NK cells from ES cells has been described elsewhere (32, 33).

### *NK cell culture*

CD49b$^+$ splenocytes were isolated from 6- to 8-wk- old C57BL/6 mice using an EasySep panNK positive selection kit (StemCell Technologies). Cells were cultured for 7 days in RPMI 1640 medium supplemented with 10% FBS, penicillin, streptomycin, $5 \times 10^{-5}$ M 2-ME (StemCell Technologies), and 100 $\mu$g/ml IL-2 (PeproTech). Flow cytometric analysis confirmed that >95% of cells generated this way were NK1.1$^+$CD3$^-$.

### *RT-PCR*

RNA from ES cells or ES-derived NK cells was isolated with a Qiagen RNeasy Mini Kit and reverse transcribed into cDNA using a Qiagen Omniscript Reverse Transcription Kit. Primer sequences were as follows: talin1 FERM domain (forward), 5′-TTGTGGGCAGATGAGTGAAA-3′, (reverse) 5′-TAGGTGTGCGTAGTGTGTG-3′ and talin2 FERM domain (forward), 5′-GCCGAGAAGCGAATATTTCA-3′, (reverse) 5′-CAC TCTCCGGTGAGGACTTC-3′.

### *H60-Fc and CD160-Fc fusion proteins*

CD160-Fc fusion protein has been previously described (34). H60 cDNA was generated by RT-PCR using RNA isolated from BALB/c mouse splenocytes, subcloned into pBluescript, and sequenced. The cDNA encoding the extracellular domain of H60 was PCR amplified, sequenced, and subcloned into the pIG vector (35). H60-Fc fusion protein was produced and purified as described for CD160-Fc fusion protein (34).

### *Cell adhesion assay*

LFA-1-mediated cell adhesion to immobilized sICAM-1 was assayed as described elsewhere (31). For adhesion of NK cells to YAC-1 cells, microwells were coated with 0.05% poly-L-lysine (PLL; Sigma-Aldrich) for 1 h at room temperature, then washed with PBS. YAC-1 cells ($10^5$/well) were dispensed into PLL-coated wells, centrifuged at 1500 rpm for 5 min, and unbound cells were washed away. This generated a confluent monolayer of YAC-1 cells. The binding of NK cells to the YAC-1 cell monolayer was tested as described for adhesion to ICAM-1-coated plates.

### *Cytotoxicity assays*

YAC-1 target cells were labeled with a Vybrant CFDA SE Cell Tracer kit (Invitrogen and Molecular Probes). CFSE-labeled YAC-1 ($10^4$) cells were mixed at varying ratios with NK cells in RPMI 1640 and 10% FBS. When talin-KO NK cells were used as effectors, $MnCl_2$ was added to a final concentration of 1 mM after mixing of effectors and targets. After 4 h, cells were washed and stained with 5 $\mu$g/ml propidium iodide and analyzed by flow cytometry. The level of cytotoxicity was determined as the number of CFSE$^+$ cells stained with propidium iodide minus the background level (as determined by target cells incubated without effectors). For cytotoxicity of L cells, target cells were trypsinized, harvested, labeled with calcein acetoxymethyl ester (calcein AM; Invitrogen and Molecular Probes), resuspended in DMEM plus 5% FBS with penicillin and streptomycin, plated in 96-well plates at $10^4$/well, and grown overnight as a monolayer. The following day targets were counted and NK cells were added at various ratios. Where appropriate, target cells were preincubated with anti-H2K Ab for 10 min before the addition of NK cells. Where appropriate, NK cells were preincubated with anti-CD44 Ab before their addition to target cells. After 4 h, cells were washed and fluorescence was measured by CytoFluor 2300 (Millipore). Specific cell lysis was calculated as a ratio of fluorescence of remaining targets to fluorescence of targets incubated without effectors (minus background).

### *Pyk2 immunoprecipitation and Western blotting*

Polystyrene 60-mm petri dishes (BD Falcon) were coated with 10 $\mu$g/ml sICAM-1 in Adhesion Buffer (20 mM Tris-HCl and 150 mM NaCl (pH 8.2)) for 1 h at room temperature. Coated plates were washed three times with PBS before use. NK cells were harvested, resuspended in prewarmed RPMI 1640 and 10% FCS at $7 \times 10^6$ cells/ml, and 0.5 ml of cell suspension was added to each plate. After cells were allowed to settle, 0.5 ml of

[3] Abbreviations used in this paper: MTOC, microtubule organizing center; PLL, poly-L-lysine; ES, embryonic stem; WT, wild type; KO, knockout; calcein AM, calcein acetoxymethyl ester; sICAM-1, soluble ICAM-1.

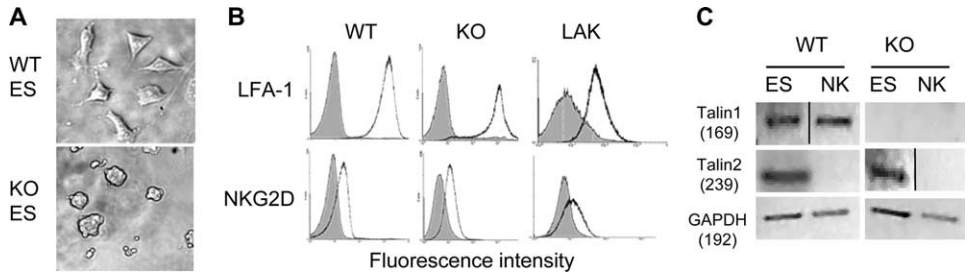


**FIGURE 1.** Expression of LFA-1, NKG2D, talin1, and talin2 in ES cells and ES-derived NK cells. *A,* WT and talin-KO ES cells were grown for 2 days on gelatinized flasks in the presence of LIF and their morphologies were examined by a phase-contrast microscope. *B,* NK cells generated from WT and talin-KO ES cells as well as IL-2-activated splenic NK cells were stained with mAbs to LFA-1 and NKG2D and analyzed by FACS. Gray histograms show staining with isotype-matched control Ab and open histograms show staining with anti-LFA-1 or anti-NKG2D. Results shown are representative of three independent experiments. *C,* RNA was isolated from WT and talin-KO ES cells and NK cells generated from the ES cells, and expression of talin1 and talin2 mRNA was determined by RT-PCR using primers specific for the FERM domain of talin1 or talin2.

prewarmed medium with or without 2 mM $MnCl_2$ was added to each plate and plates were incubated at 37°C for 20 min, washed twice with 1 ml of prewarmed RPMI 1640 and 10% FCS, and then cells were lysed with 1 ml of ice-cold lysis buffer (10 mM Tris-HCl (pH 8.0), 150 mM KCl, 1 mM EDTA (pH 8.0), 1% Triton X-100, 0.5% BSA, 1 mM $Na_3VO_4$, 1 mM PMSF, 5 $\mu$g/ml aprotinin, 10 $\mu$g/ml leupeptin, and 10 $\mu$g/ml pepstatin). For control samples, 3.5 million NK cells were lysed in a microfuge tube. Control samples corresponding to cells bound to ICAM-1 in the presence of $Mn^{2+}$ were lysed in the presence of 1 mM $MnCl_2$. Immunoprecipitation was conducted as described previously (34).

### *Confocal microscopy*

Polystyrene beads were coated with 20 $\mu$g/ml sICAM-1, 20 $\mu$g/ml H60-Fc, or 0.005% PLL, spun down and blocked in 200 $\mu$g/ml BSA, then washed and resuspended in RPMI 1640 and 10% FBS. NK cells were harvested and resuspended in RPMI 1640 plus 10% FBS. In brief, $10^5$ beads and $2.5 \times 10^5$ cells were gently mixed in an Eppendorf tube and, where appropriate, $MnCl_2$ was added to a final concentration of 1 mM. After 5 min, cell-bead conjugates were gently resuspended, dropped onto poly-L-lysine coated coverslips, and incubated for various time points. Coverslips were fixed with 4% formaldehyde and samples were permeabilized with Hanks' saponin solution (HBSS containing 2% FBS, 5 mM EDTA, and 0.5% saponin). Actin was detected by staining samples fixed on coverslips in a 1/40 dilution of rhodamine phalloidin or Alexa Fluor 647 phalloidin in Hanks' saponin solution. Talin, phospho-Pyk2, and granzyme B were stained by incubating samples fixed on coverslips for 1 h in a 1/40 dilution in Hanks' saponin solution of the corresponding primary Ab. Coverslips were washed three times with Hanks' saponin solution and then stained at room temperature for 1 h with 10 $\mu$g/ml Alexa Fluor 488-conjugated goat anti-mouse IgG Ab for talin and phospho-Pyk2- or Alexa Fluor 568-conjugated donkey anti-rabbit IgG Ab for granzyme B. Coverslips were washed three times with Hanks' saponin solution and once with HBSS, then mounted with Vectashield mounting medium (Vector Laboratories). Actin-stained cell-bead conjugates were analyzed using a Leica TCS2 confocal system with a ×100 objective lens, zoom 4. All other cell-bead conjugates were analyzed using a Nikon C1-si confocal microscope with a ×100 objective lens, zoom 4. Images were collected using sequential scanning to avoid bleed-through. Images were processed and merged using Volocity software (Improvision) and exported as JPG files. For quantification of fluorescent intensity at the site of binding, the sum intensity in the channel of interest was determined using Volocity software for the area of contact between a cell and a bead and compared with the sum fluorescent intensity of the whole same cell using the following equation: [sum intensity (contact site)/sum intensity (whole cell)] × 100. For the comparison of phospho-Pyk2 intensity, fluorescent intensity of unbound cells and cells bound to beads was determined using Volocity software. All images used for this analysis were collected from the same experiment using the same instrument settings. The average fluorescent intensity of unbound WT cells was normalized to 1 and all other values are expressed relative to this.

### *Statistics*

Student's two-tailed *t* test was used for comparison of sets of matched samples. Grouped samples were analyzed using one-way ANOVA.

## Results

### *In vitro generation of NK cells from talin1-deficient ES cells*

Since homozygous *Tln1* KO in mice results in embryonic lethality (36), we generated NK cells from *Tln1*$^{-/-}$ ES cells (clone A28) and the corresponding WT ES cells (clone HM1) by in vitro differentiation cultures as previously described (32, 33). As reported previously (28), the two ES cell lines exhibited different morphologies. WT ES cells attached firmly to gelatin-coated plates, flattened, and spread, whereas talin-KO ES cells did not spread and appeared rounded (Fig. 1*A*). Flow cytometric analysis showed that NK cells generated from WT and talin-KO ES cells expressed similar levels of LFA-1 and the NK cell receptor NKG2D (Fig. 1*B*). The level of LFA-1- on ES-derived NK cells was significantly higher than that of IL-2-stimulated splenic NK cells, whereas the level of NKG2D was comparable.

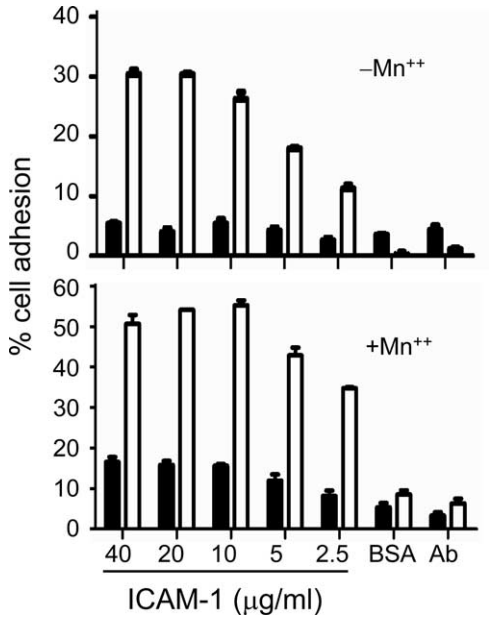


**FIGURE 2.** Adhesion to immobilized ICAM-1. WT NK cells (□) or talin-KO NK cells (■) were incubated without (*top panel*) or with (*bottom panel*) 1 mM $Mn^{2+}$. Cells were incubated on varying concentrations of immobilized soluble ICAM-1 as described in *Materials and Methods*. For control adhesion, BSA was immobilized in place of ICAM-1. For specificity control, cells were incubated with anti-LFA-1-blocking Ab. Results shown are representative of three independent experiments, each done in triplicate. Error bars indicate SEM.

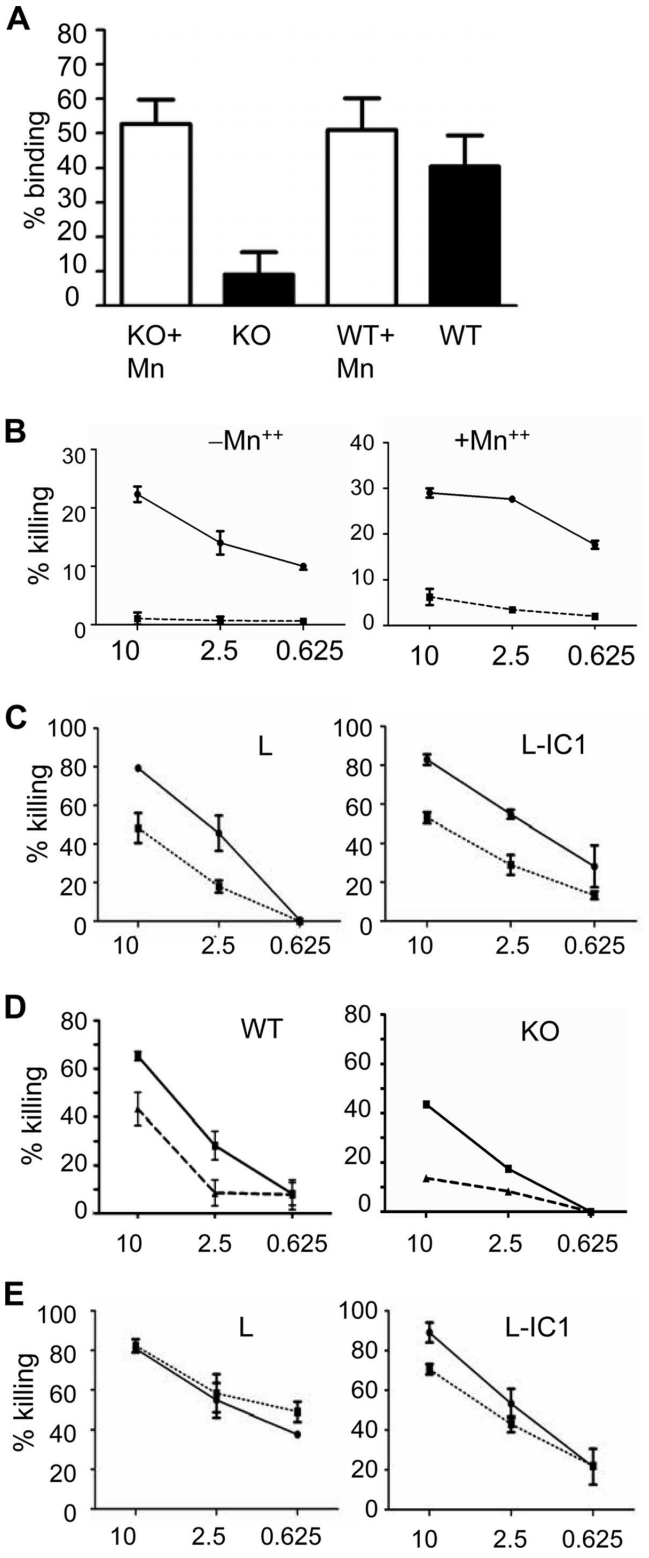


**FIGURE 3.** Cytotoxicity of WT and talin-KO NK cells against YAC-1 and fibroblast targets. *A,* WT or talin-KO NK cells were labeled with calcein AM and binding to monolayers of YAC-1 cells was tested in the presence (□) or absence (■) of 1 mM $Mn^{2+}$. The percentages of NK cells bound to YAC-1 monolayers were determined as in Fig. 2. Results shown are representative of three experiments, each done in triplicate. Error bars indicate SEM. *B,* Cytotoxicity against YAC-1 target cells was analyzed by FACS. YAC-1 targets were labeled with CFDA-SE and incubated for 4 h with talin-KO (dashed line) or WT (solid line) NK cells. Following incubation, cells were washed and analyzed by flow cytometer as described in *Materials and Methods*. Results shown are representative of three independent experiments, each done in triplicate. Error bars indicate SEM. *C,* L cell fibroblasts (*left panel*) or ICAM-1-transfected L cells (*right panel*) were labeled with calcein AM and grown in a monolayer overnight. Talin-KO (dashed line) or WT (solid line) were incubated for 4 h with L or L-IC1 cells. Fluorescence was read and specific cell lysis was determined as described in *Materials and Methods*. Results shown are representative of three independent experiments, each done in triplicate. Error bars indicate SEM. *D,* L cells were labeled with calcein AM and grown in a monolayer overnight. WT *(left panel)* or talin-KO (*right panel*) NK cells were treated with (dashed line) or without (solid line) anti-CD44-blocking Ab, then incubated for 4 h with target cells. Fluorescence was read and specific lysis was determined as described in *Materials and Methods*. Results shown are representative of three independent experiments, each done in triplicate. Error bars indicate SEM. *E,* L cell fibroblasts (*left panel*) or ICAM-1-transfected L cells (*right panel*) were labeled with calcein AM and grown in a monolayer overnight. Talin-KO (dashed line) or WT (solid line) cells were incubated for 4 h with L or L-IC1 cells following incubation of target cells with anti-H2K Ab to induce Ab-mediated cellular cytotoxicity. Fluorescence was read and specific cell lysis was determined as described in *Materials and Methods*. Results shown are representative of three independent experiments, each done in triplicate. Error bars indicate SEM.

A second talin gene, *Talin2*, has been identified in mice (37). Although its function is still unknown, the sequence of *Talin2* is very similar to that of *Talin1* and the talin2 protein is predicted to have a similar function to talin1, with the FERM domain and actin and integrin binding sites being conserved between the two (37). Although talin1 mRNA is widely expressed in various tissues, the expression of talin2 mRNA is more restricted and is undetectable in hematopoietic cells (37). RT-PCR analysis of WT and talin1-KO ES cells as well as NK cells derived from them using primers specific for the FERM domains of talin1 and talin2 showed that talin-KO ES cells and NK cells generated from them did not express talin1 mRNA. Talin2 mRNA was detectable in both WT and talin-KO ES cells but not in ES-derived NK cells (Fig. 1*C*). Therefore, it is unlikely that talin2 will be able to compensate functionally for talin1 deficiency in NK cells, and hence these cells are referred to subsequently as talin-KO NK cells.

### *Talin is required for LFA-1-mediated cell adhesion*

To test the effect of talin deficiency on LFA-1-mediated cell adhesion, binding of NK cells generated from WT and talin-KO ES cells was tested using microwells coated with increasing concentrations of recombinant sICAM-1. WT NK cells without prior activation adhered to immobilized ICAM-1 in a dose-dependent manner and anti-LFA-1 Ab abrogated the binding, confirming that cell adhesion to ICAM-1 is mediated by LFA-1. In addition, cells showed little or no (<1%) nonspecific adhesion to BSA (Fig. 2, *top panel*). In contrast, the level of adhesion of talin-KO NK cells to ICAM-1 at any concentration tested was not significantly higher than that of nonspecific adhesion to BSA and anti-LFA-1 had no effect, indicating that LFA-1-mediated adhesion of talin-KO NK cells is severely impaired.

Manganese is known to bind to the extracellular domain of LFA-1 and locks it in a conformation with maximal affinity for its ligand independent of inside-out signaling (38, 39). Therefore, we tested the adhesion of ES-derived NK cells to ICAM-1 in the presence of 1 mM $Mn^{2+}$. Treatment of WT NK cells with 1 mM $Mn^{2+}$ significantly increased their adhesion to ICAM-1 (Fig. 2, *bottom panel*). Talin-KO NK cells also adhered to ICAM-1 in the presence of 1 mM $Mn^{2+}$, although the level of adhesion was significantly lower than that of WT NK cells treated or not with $Mn^{2+}$. Thus, $Mn^{2+}$ seems to activate LFA-1 on talin-KO NK cells, but it does

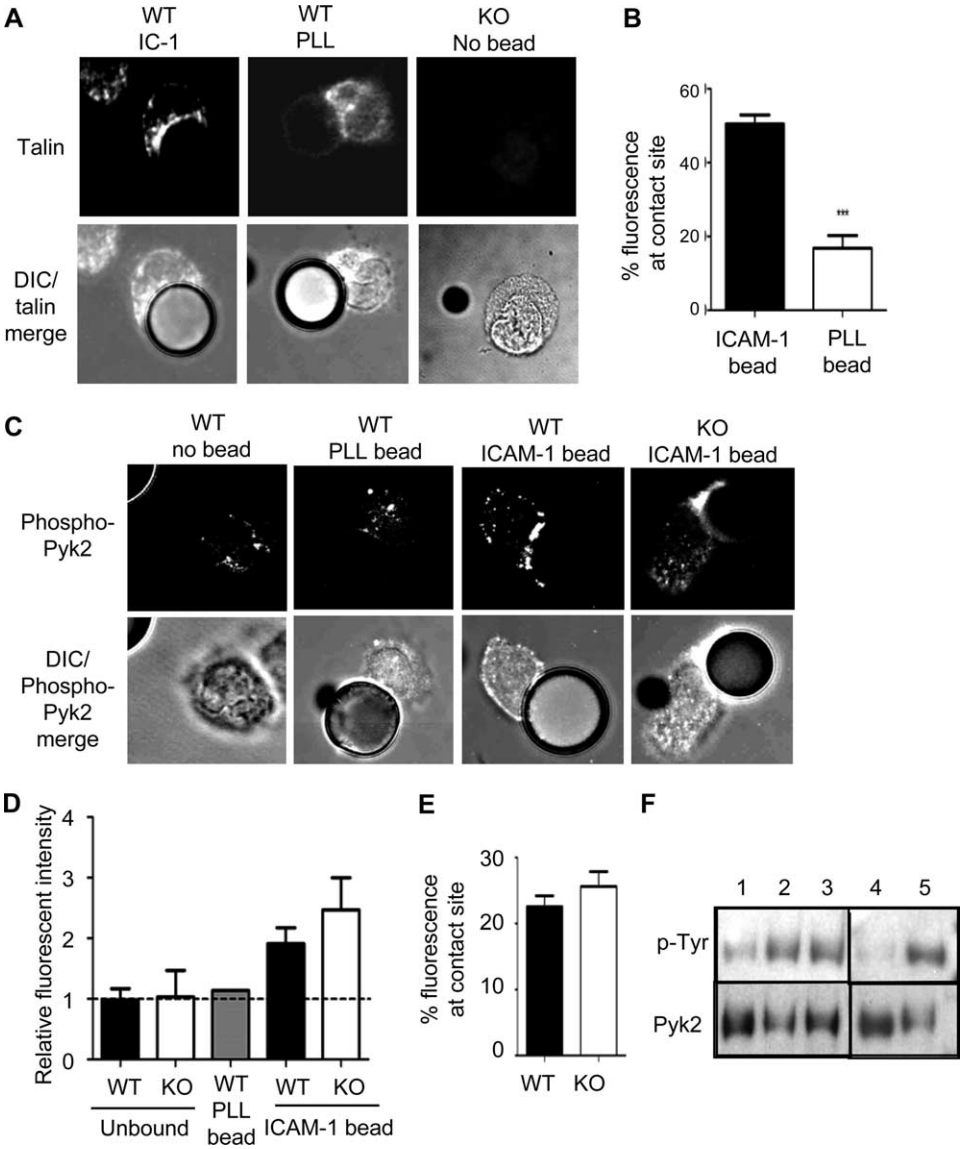


**FIGURE 4.** Binding of LFA-1 to ICAM-1 induces accumulation of talin and phosphorylation and localization of Pyk2. Polystyrene beads were coated with ICAM-1 or PLL as described in *Materials and Methods*. *A,* WT NK cells (*left two panels*) were incubated with bead and then fixed, permeabilized, and stained at 20°C with anti-talin mAb and Alexa Fluor 488 secondary Ab. Staining of talin-KO cells with anti-talin Ab confirmed a lack of talin expression (*right panel*; $n = 18$ per condition). *B,* Fluorescent intensity of talin staining at the contact site between a WT cell and an ICAM-1-coated bead (■) or a PLL-coated bead (□) was expressed as a percentage of total fluorescent intensity of talin staining within the cell. Error bars represent SEM; $p < 0.001$, $n = 13$ per condition. *C,* WT (*left three panels*) or talin-KO (*right panel*) NK cells were incubated with beads and then fixed, permeabilized, and stained at 20°C with anti-phospho-Pyk2 mAb and Alexa Fluor 488 secondary Ab. Talin-KO cells were incubated in the presence of 1 mM $Mn^{2+}$ to induce binding to beads. $n = 30$ per condition and represent at least three independent experiments. *D,* Fluorescence intensity of phospho-Pyk2 staining was measured for WT (black bars) and talin-KO (□) cells unbound to beads and normalized to 1, then compared with fluorescent intensity of cells bound to ICAM-1- coated beads. Error bars indicate SEM; $n = 10$ per condition. *E,* Fluorescent intensity of phospho-Pyk2 staining at the contact site between a WT (■) and a talin-KO (□) cell and an ICAM-1-coated bead was expressed as a percentage of total fluorescent intensity of phospho-Pyk2 staining within the cell. Error bars represent SEM; $p = 0.285$, $n = 15$ per condition. *F,* WT (*lanes 1–3*) and talin-KO NK cells (*lanes 4* and *5*) were allowed to bind to polystyrene petri dishes coated with soluble ICAM-1 at 37°C in the presence (*lanes 3–5*) or absence (*lanes 1* and *2*) of 1 mM $Mn^{2+}$. Control samples not incubated on plates (*lanes 1* and *4*) were lysed in a microfuge tube with ice-cold lysis buffer. Pyk2 was immunoprecipitated as described in *Materials and Methods*. Immunoprecipitated samples were divided in half and analyzed for Pyk-2 (loading control) and phosphotyrosine by immunoblotting using anti-Pyk-2 and anti-phosphotyrosine (4G10) primary Abs, respectively. Microscopy images were collected by confocal microscopy using sequential scanning to avoid bleed-through and imported into Volocity software (Improvision). Images were merged in Volocity and exported as JPG files. Original magnification was ×400 for all images shown. DIC, Differential interference contrast.

not fully compensate for talin deficiency in LFA-1-mediated cell adhesion to purified and immobilized ICAM-1.

### *Talin-KO$^-$ NK cells are unable to mediate cytotoxicity against conventional targets but are able to kill fibroblasts*

To test the effects of talin deficiency on NK cell cytotoxicity, we first tested whether talin-KO NK cells bind to YAC-1 cells in the presence or not of 1 mM $Mn^{2+}$. YAC-1 cells were immobilized in PLL-coated microwells, and NK cells labeled with calcein AM were incubated with targets. WT NK cells bound to YAC-1 cells in the absence of $Mn^{2+}$ and 1 mM $Mn^{2+}$ enhanced the binding. Talin-KO NK cells did not efficiently bind to YAC-1 without $Mn^{2+}$, but they bound to YAC-1 cells to a similar level to WT cells in the presence of 1 mM $Mn^{2+}$ (Fig. 3*A*). It should be noted

that YAC-1 cells expressed LFA-1 and NK cells expressed ICAM-1, which likely contributed to the formation of cell aggregates. As expected from the results with conjugate formation, WT NK cells killed YAC-1 cells, whereas talin-KO NK cells did not kill YAC-1 in the absence of $Mn^{2+}$. Upon addition of $Mn^{2+}$, the killing of YAC-1 by WT NK cells was slightly enhanced, whereas talin-KO NK cells did not significantly kill YAC-1 despite efficient binding to YAC-1 cells (Fig. 3*B*).

To further test the effects of talin deficiency on NK cell cytotoxicity, the murine fibroblast line L cells, which do not express ICAM-1, and ICAM-1-transfected L cells (L-IC1) (29) were used as target cells. Unexpectedly, talin-KO NK cells efficiently killed L cells in the absence of exogenous $Mn^{2+}$. ICAM-1 expression on L cells enhanced the cytotoxicity (Fig. 3*C*). In addition, WT cells were able to mediate cytotoxicity against untransfected L cells. The cytotoxicity of talin-KO NK cells against both L cells and L-IC1 cells was slightly lower than that of WT NK cells. These results suggest that killing of L cells is mediated by both talin-dependent and talin-independent mechanisms. Since CD44 has been shown to contribute to NK cell cytotoxicity (1), we tested the effects of anti-CD44 mAb on the cytotoxicity against L cells. Anti-CD44 mAb significantly reduced the cytotoxicity of both WT and talin-KO NK cells against L cells (Fig. 3*D*). These results indicate that talin-KO NK cells are able to kill L cells by a CD44-dependent mechanism. The incomplete inhibition by anti-CD44 mAb suggests that other receptors may also mediate killing of L cells.

We also tested the effect of talin deficiency on CD16-mediated Ab-dependent cell-mediated cytotoxicity. Because L cells uniformly express the MHC class I H-$2K^k$, they were coated with anti-H-$2K^k$ mAb before incubation with effector cells. Both WT and talin-KO NK cells killed L cells very efficiently, and the expression of ICAM-1 on L cells did not enhance the cytotoxicity (Fig. 3*E*). Thus, talin-KO NK cells are capable of killing target cells by LFA-1-independent mechanisms.

### *Binding of NK cells to ICAM-1-coated beads results in recruitment of talin and Pyk2 phosphorylation*

Although the above results showed that talin is required for LFA-1-mediated NK cell adhesion, talin may have an additional role in NK cell cytotoxicity, because talin-KO NK cells are unable to kill YAC-1 even when they efficiently form conjugates in the presence of $Mn^{2+}$. To further study the effects of talin deficiency in NK cell activation, we used cell-size polystyrene beads coated with sICAM-1 as an artificial target, which allowed us to study LFA-1-mediated outside-in signaling in NK cells independent of other NK cell receptors. Flow cytometric analysis showed that the density of ICAM-1 on the coated beads in this study was comparable to that of mouse lymphoid tumor cell lines (data not shown). As a negative control, we also prepared PLL-coated beads. Both ICAM-1-coated beads and control beads readily bound to WT NK cells. Bead-NK cell conjugates were fixed, permeabilized, stained for talin, and analyzed by confocal microscopy. In WT NK cells binding control beads, talin was distributed throughout the cytosol, with 16.8 ± 3% (mean ± SEM; $n = 18$) of talin found at the site of contact, whereas 50.4 ± 2.4% ($n = 18$) of talin accumulated at the point of contact with an ICAM-1-coated bead (Fig. 4, *A* and *B*). Talin-KO NK cells were not stained with anti-talin mAb, confirming the specificity of the staining. Thus, binding of ICAM-1 to LFA-1 seems to induce translocation of talin from the cytosol to the site of LFA-1 ligation.

LFA-1 ligation has been shown to rapidly induce phosphorylation of the protein tyrosine kinase Pyk2, although the precise role of Pyk2 in NK cell activation is still unclear (7, 40). When we stained ES-derived NK cells with an anti-phospho-Pyk2 Ab that

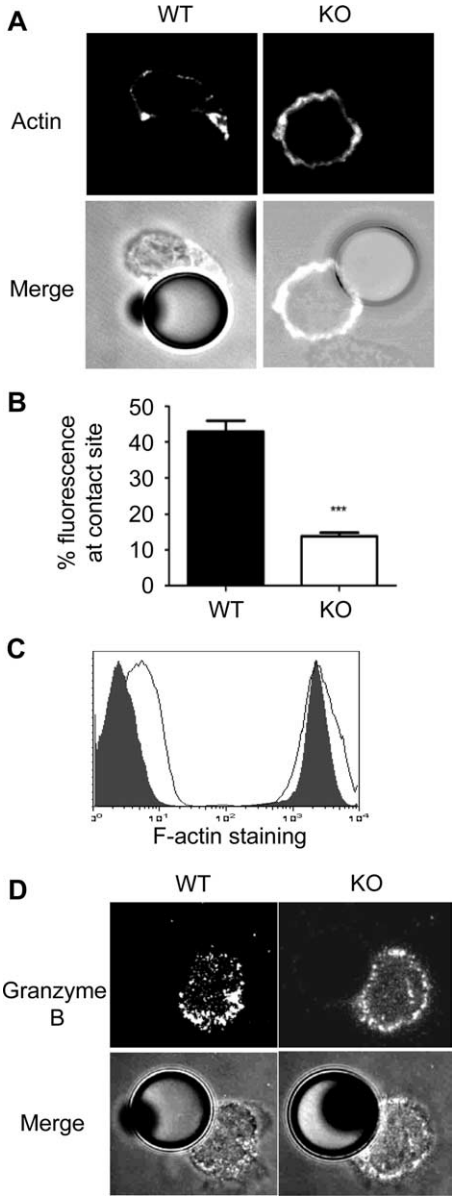


**FIGURE 5.** Engagement of LFA-1 to ICAM-1 results in talin-dependent actin accumulation, but not accumulation of cytotoxic granules. Polystyrene beads were coated with ICAM-1 or poly-L-lysine as described in *Materials and Methods*. *A,* WT (*left panel*) or talin-KO (*right panel*) NK cells were incubated with ICAM-1-coated beads (talin-KO cells were incubated in the presence of 1 mM $Mn^{2+}$ to facilitate binding to beads). Cells were fixed with formaldehyde, permeabilized, and stained at 20°C with rhodamine phalloidin. $n = 50$ images per condition and represent at least three independent experiments. Images were collected by a Leica TCS2 confocal microscope using sequential scanning to avoid bleed-through and imported into Volocity software (Improvision). Images were merged in Volocity and exported as JPG files. Original magnification ×400 for all images is shown. *B,* Fluorescent intensity of actin staining at the contact site between a WT cell (■ or a talin-KO cell (□) was expressed as a percentage of total fluorescent intensity of actin staining within the cell. Error bars represent SEM; $n = 22$ (WT) and 28 (KO); $p = < 0.0001$. *C,* WT (solid line) or talin-KO (filled histogram) NK cells were stained with phalloidin Alexa Fluor 647 and analyzed by FACS to determine total F-actin content. Histograms of unstained control cells are also shown. *D,* WT (*bottom panel*) or talin-KO (*top panel*) NK cells were incubated with ICAM-1-coated beads (talin-KO cells were incubated in the presence of 1 mM $Mn^{2+}$ to facilitate binding to beads). Cells were fixed with formaldehyde, permeabilized, and stained with anti-granzyme B mAb and Alexa Fluor 568 secondary Ab; $n = 28$ per condition and represent at least three independent experiments. Images were collected and processed by confocal microscopy as in Fig. 4.

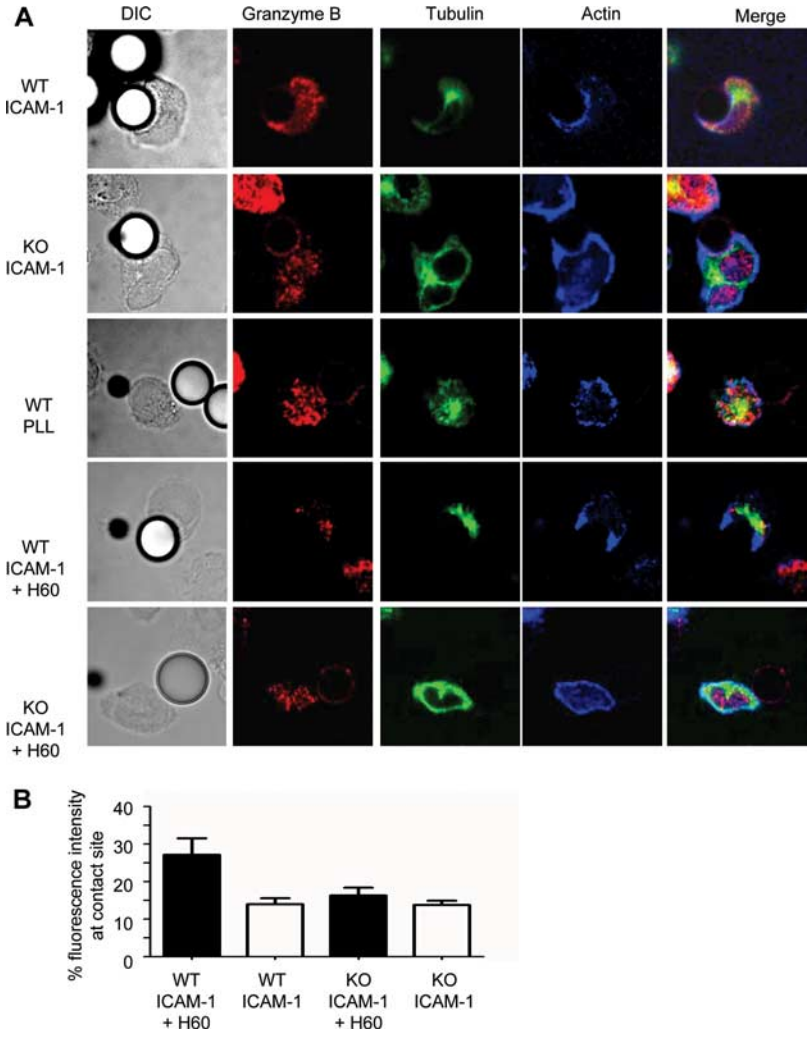


**FIGURE 6.** Coengagement of LFA-1 and NKG2D results in polarization of actin, cytotoxic granules, and the MTOC. *A,* WT or talin-KO NK cells were incubated with beads coated with sICAM-1, sICAM-1 and H60-Fc, or PLL. Talin-KO cells were incubated in the presence of 1 mM $Mn^{2+}$ to facilitate binding to beads. Cells were fixed with formaldehyde, permeabilized, and stained at 20°C with anti-granzyme B mAb with Alexa Fluor 568 secondary Ab, anti-$\beta$-tubulin mAb with Alexa Fluor 488 secondary Ab, and Alexa Fluor 647 phalloidin. *B,* Fluorescent intensity of granzyme B staining at the contact site between a WT cell or a talin-KO cell was expressed as a percentage of total fluorescent intensity of granzyme B staining within the cell. Error bars represent SEM; $n = 8–16$ per condition. Images were collected by confocal microscopy and processed as in Fig. 4.

specifically recognizes activated Pyk2 phosphorylated at $Tyr^{402}$ (41, 42), the level of phospho-Pyk2 in both WT and talin-KO NK cells was low (Fig. 4, *C* and *D*). Upon binding of ICAM-1-coated beads to WT NK cells, the overall level of phospho-Pyk2 increased 2-fold (Fig. 4*D*) and >20% of the staining localized to the site of bead binding in 72% ($n = 30$) of the conjugates (Fig. 4*E*). Binding of WT cells to a PLL-coated bead did not result in this localization. Talin-KO NK cells, upon treatment with 1 mM $Mn^{2+}$, bound the beads and showed a similar increase in the overall level of phospho-Pyk2 as WT NK cells (Fig. 4, *D* and *E*). Phospho-Pyk2 also accumulated at the site of contact with the bead in 70% of the conjugates ($n = 30$). To further quantitate Pyk2 phosphorylation following binding to ICAM-1, WT and talin-KO NK cells (in the presence of 1 mM $Mn^{2+}$) were incubated on ICAM-1-coated plates. Pyk2 was immunoprecipitated and phosphorylation was detected by western blotting (Fig. 4*F*). Pyk2 phosphorylation increased in both WT and talin-KO cells relative to control cells that had not been bound to plates. $Mn^{2+}$ did not affect Pyk2 phosphorylation in WT cells. Thus, LFA-1 ligation generates outside-in signals, leading to Pyk2 phosphorylation at the site of LFA-1 ligation, and this process is talin independent. In addition, the phosphorylation and localization of Pyk2 following binding of talin-KO cells to ICAM-1-coated beads indicates that binding of these cells in the presence of $Mn^{2+}$ is LFA-1 dependent and not due to nonspecific interactions.

*Talin is required for actin accumulation in NK cells binding ICAM-1-coated beads*

We tested the effect of talin disruption on actin accumulation in NK cells binding ICAM-1-coated beads. WT NK cells, upon binding ICAM-1-coated beads, flattened and formed a lamellipodia-like structure, which wrapped around the bead, and F-actin accumulated at the lamellipodia-like structure (Fig. 5*A*, *bottom panel*). The actin accumulation was seen as early as 5 min after the initiation of the incubation and persisted for >30 min. Although talin-KO NK cells pretreated with 1 mM $Mn^{2+}$ readily bound ICAM-1-coated beads, they remained round, with F-actin evenly distributed around the edge of the cell. Longer incubation times did not result in actin accumulation in talin-KO NK cells (results not shown). In WT NK cells, >40% of F-actin could be found at the contact site (42.9 ± 3%, $n = 22$). Talin-KO NK cells showed significantly less, ~15% of total actin (13.9 ± 0.9%, $n = 28$), at the contact site (Fig. 5*B*). This difference in fluorescence intensity likely reflects both a decrease in accumulation and, to a certain extent, a decreased contact area at the contact site due to the rounded phenotype of talin-KO cells. Because talin contains multiple binding sites for cortical F-actin, it is conceivable that a talin deficiency may result in lower overall levels of F-actin within talin-KO NK cells. However, comparable levels of F-actin were detected in WT and talin-KO by FACS (Fig. 5*C*). Although binding of WT cells to an ICAM-1-coated bead caused actin

accumulation, staining for granzyme B showed granules dispersed throughout the cell in both WT and KO (with $Mn^{2+}$) NK cells (Fig. 5*D*). Taken together, these results show the importance of LFA-1 signaling in actin accumulation and the critical role that talin plays in this signaling.

### *NKG2D ligation induces talin-dependent polarization of cytotoxic granules toward targets*

The stimulatory NK cell receptor NKG2D is known to mediate NK cell cytotoxicity against many tumors. Therefore, we tested the effects of NKG2D ligation on cytotoxic granule translocation in WT and talin-KO NK cells. H60 is a ligand for NKG2D (8). We generated H60-Fc fusion protein and immobilized it on cell-size beads to ligate NKG2D. An unrelated Fc fusion protein, CD160-Fc (34), was used as a negative control. Beads were coated with sICAM-1 and H60-Fc (20 $\mu$g/ml each). Binding of ICAM-1/H60-Fc beads to WT NK cells resulted in a marked accumulation of granzyme B at the point of contact with the bead. As expected, F-actin accumulated at the site and the MTOC also polarized toward the beads. Thus, the merged image of NK cells stained for granzymes (red), tubulin (green), and F-actin (blue) showed colocalization of these proteins at the site of bead binding (Fig. 6*A*). In contrast, following binding of ICAM-1/H60-Fc-coated beads to talin-KO cells in the presence of $Mn^{2+}$, granzyme B was dispersed throughout the cells, MTOC was in a random position, and F-actin remained evenly distributed around the cell periphery. Control beads coated with ICAM-1 and CD160-Fc did not induce granzyme B polarization, indicating that cytotoxic granule polarization induced by H60-Fc is not due to CD16 ligation by the Fc portion of the fusion proteins (data not shown). To quantify granule polarization, we measured the fluorescence intensity of anti-granzyme B staining at the site of bead binding and compared it with the overall fluorescence intensity of the cell (Fig. 6*B*). In WT NK cells, binding beads coated with ICAM-1 and H60, ~30% ($27 \pm 4.4\%$, $n = 7$) of the fluorescence intensity of the granzyme B staining was at the point of contact, whereas those cells in contact with ICAM-1 beads had ~14% ($14.0 \pm 1.5\%$, $n = 8$) of fluorescence intensity at the contact site. With talin-KO NK cells, the fluorescence intensity at the point of contact with beads was low regardless of whether the beads were coated with ICAM-1 alone ($13.8 \pm 1.1\%$, $n = 8$) or ICAM-1 and H60 ($16.3 \pm 2\%$, $n = 16$). Thus, activating signals from NKG2D causes granzyme polarization in WT cells but this polarization requires talin, presumably because talin-dependent reorganization of the actin cytoskeleton is required for this process.

## Discussion

In this study, we have generated NK cells from talin1-KO ES cells and studied the role of talin in NK cell cytotoxicity. Our results have shown that the cytotoxicity of talin-KO NK cells is impaired and suggest a dual role for talin. First, talin seems to act as an activator of LFA-1, because talin-KO NK cells are unable to adhere to ICAM-1. Second, talin is also required for LFA-1-induced reorganization of the actin cytoskeleton in NK cells, which is required for polarization of cytotoxic granules toward target cells. Thus, talin is required for not only inside-out activation of LFA-1 but also for outside-in signaling through LFA-1 leading to NK cell polarization.

Talin has been shown to be required for activation of $\beta_1$ and $\beta_3$ integrins (22, 23, 25). Overexpression of the talin head also induces changes in LFA-1 conformation (22). Talin knockdown in Jurkat T cells and peripheral blood T cells also showed a requirement for talin in TCR-induced LFA-1 activation (43). Thus, activation of LFA-1 by talin is required for effective LFA-1-mediated cell adhesion. However, the addition of exogenous $Mn^{2+}$ to Jurkat cells in which talin is knocked down is unable to rescue the defect in adhesion (43). In our study, exogenous $Mn^{2+}$ only partially restores LFA-1-mediated adhesion of talin-KO NK cells. Since the activation of LFA-1 by $Mn^{2+}$ is thought to be independent of endogenous signaling, it seems likely that effective LFA-1-mediated cell adhesion requires not only high-affinity conformation of LFA-1 but also talin-dependent actin accumulation and LFA-1 clustering, as observed for other integrins (44, 45).

Although LFA-1-ICAM-1 interaction is sufficient for actin reorganization in NK cells, a second signal is required for granule polarization and reorientation of the MTOC. Coligation of LFA-1 and NKG2D induces polarization of cytotoxic granules and MTOC toward the targets. Interestingly, ligation of NKG2D alone has no effect (data not shown). Furthermore talin-KO NK cells do not show polarization of granules and MTOC upon coligation of LFA-1 and NKG2D. Therefore, polarization of the actin cytoskeleton is likely required for MTOC and granule polarization. This is consistent with previous studies in which disruption of actin dynamics by inhibitors prevents MTOC reorientation (46). Our results also show differential effects of activation signals through LFA-1 and NKG2D in NK cells. LFA-1 signals induce actin reorganization but not granule and MTOC polarization, whereas NKG2D signals induce polarization of granules and MTOC, but not actin reorganization. In contrast to our results with ES-derived NK cells and IL-2-activated splenic NK cells (data not shown), Barber et al. (5) showed that LFA-1 ligation on resting human NK cells results in polarization of perforin-containing granules toward a target cell or ICAM-1-coated beads. The reason for the difference between our results and those of Barber et al. (5) is still unknown. Nevertheless, ligation of LFA-1 leads to reorganization of the actin cytoskeleton in both studies and our results implicate a critical role for talin in this process.

In T cells, LFA-1 ligation has been shown to induce Vav1 phosphorylation, which leads to activation of WASp and Arp2/3 resulting in actin polymerization (47). Although LFA-1 ligation also induces phosphorylation and activation of Pyk2, it is unlikely responsible for Vav1 phosphorylation, because our results have shown that Pyk2 phosphorylation is talin independent, whereas reorganization of the actin cytoskeleton requires talin. Talin is known to interact with multiple proteins, including actin and also vinculin, which in turn associates with paxillin (48) and $\alpha$-actinin (49). Paxillin functions as a scaffold protein and associates with a number of signaling proteins (13). Thus, talin likely forms a multiprotein complex as it associates with LFA-1 and recruits signaling proteins yet to be identified that are responsible for reorganization of the actin cytoskeleton.

Whereas LFA-1-dependent NK cytotoxicity is impaired by talin deficiency, NK cells are able to kill fibroblast L cells in an LFA-1/talin-independent manner. CD44 has been reported to compensate for LFA-1 deficiency in NK cytotoxicity, since NK cells from $CD44^{+/+}LFA\text{-}1^{-/-}$ mice retained some cytotoxic function (1). Since CD44 acts as a link between the plasma membrane and the actin cytoskeleton through members of the ERM family of proteins (50), it appears that the compensatory role that CD44 plays is not limited to adhesion but extends to actin reorganization as well.

In summary, by using in vitro differentiation to generate talin-KO NK cells and protein-coated beads to investigate these cells, we have shown a dual role for talin. Talin is required both for LFA-1 activation and LFA-1-mediated actin cytoskeletal rearrangement. This study elucidates talin's role in LFA-1 function and illustrates the importance of talin for the transduction of LFA-1-mediated early signaling events in NK cell cytotoxicity.

## Acknowledgments

We thank Dr. Pauline Johnson for anti-CD44 Ab.

## Disclosures

The authors have no financial conflict of interest.

## References

1. Matsumoto, G., M. P. Nghiem, N. Nozaki, R. Schmits, and J. M. Penninger. 1998. Cooperation between CD44 and LFA-1/CD11a adhesion receptors in lymphokine-activated killer cell cytotoxicity. *J. Immunol.* 160: 5781–5789.
2. Chen, B. P., M. Malkovsky, J. A. Hank, and P. M. Sondel. 1987. Nonrestricted cytotoxicity mediated by interleukin 2-expanded leukocytes is inhibited by anti-LFA-1 monoclonal antibodies (MoAb) but potentiated by anti-CD3 MoAb. *Cell. Immunol.* 110: 282–293.
3. Hildreth, J. E., F. M. Gotch, P. D. Hildreth, and A. J. McMichael. 1983. A human lymphocyte-associated antigen involved in cell-mediated lympholysis. *Eur. J. Immunol.* 13: 202–208.
4. Suzuki, J., S. Yamasaki, J. Wu, G. A. Koretzky, and T. Saito. 2007. The actin cloud induced by LFA-1-mediated outside-in signals lowers the threshold for T-cell activation. *Blood* 109: 168–175.
5. Barber, D. F., M. Faure, and E. O. Long. 2004. LFA-1 contributes an early signal for NK cell cytotoxicity. *J. Immunol.* 173: 3653–3659.
6. Riteau, B., D. F. Barber, and E. O. Long. 2003. Vav1 phosphorylation is induced by $\beta_2$ integrin engagement on natural killer cells upstream of actin cytoskeleton and lipid raft reorganization. *J. Exp. Med.* 198: 469–474.
7. Gismondi, A., J. Jacobelli, F. Mainiero, R. Paolini, M. Piccoli, L. Frati, and A. Santoni. 2000. Cutting edge: functional role for proline-rich tyrosine kinase 2 in NK cell-mediated natural cytotoxicity. *J. Immunol.* 164: 2272–2276.
8. Malarkannan, S., P. P. Shih, P. A. Eden, T. Horng, A. R. Zuberi, G. Christianson, D. Roopenian, and N. Shastri. 1998. The molecular and functional characterization of a dominant minor H antigen, H60. *J. Immunol.* 161: 3501–3509.
9. Carayannopoulos, L. N., O. V. Naidenko, D. H. Fremont, and W. M. Yokoyama. 2002. Cutting edge: murine UL16-binding protein-like transcript 1: a newly described transcript encoding a high-affinity ligand for murine NKG2D. *J. Immunol.* 169: 4079–4083.
10. Cerwenka, A., A. B. Bakker, T. McClanahan, J. Wagner, J. Wu, J. H. Phillips, and L. L. Lanier. 2000. Retinoic acid early inducible genes define a ligand family for the activating NKG2D receptor in mice. *Immunity* 12: 721–727.
11. Diefenbach, A., J. K. Hsia, M. Y. Hsiung, and D. H. Raulet. 2003. A novel ligand for the NKG2D receptor activates NK cells and macrophages and induces tumor immunity. *Eur. J. Immunol.* 33: 381–391.
12. Bryceson, Y. T., M. E. March, H. G. Ljunggren, and E. O. Long. 2006. Activation, coactivation, and costimulation of resting human natural killer cells. *Immunol. Rev.* 214: 73–91.
13. Critchley, D. R., M. R. Holt, S. T. Barry, H. Priddle, L. Hemmings, and J. Norman. 1999. Integrin-mediated cell adhesion: the cytoskeletal connection. *Biochem. Soc. Symp.* 65: 79–99.
14. Garcia-Alvarez, B., J. M. de Pereda, D. A. Calderwood, T. S. Ulmer, D. Critchley, I. D. Campbell, M. H. Ginsberg, and R. C. Liddington. 2003. Structural determinants of integrin recognition by talin. *Mol. Cell* 11: 49–58.
15. Hemmings, L., D. J. Rees, V. Ohanian, S. J. Bolton, A. P. Gilmore, B. Patel, H. Priddle, J. E. Trevithick, R. O. Hynes, and D. R. Critchley. 1996. Talin contains three actin-binding sites each of which is adjacent to a vinculin-binding site. *J. Cell Sci.* 109: 2715–2726.
16. Ling, K., R. L. Doughman, A. J. Firestone, M. W. Bunce, and R. A. Anderson. 2002. Type I$\gamma$ phosphatidylinositol phosphate kinase targets and regulates focal adhesions. *Nature* 420: 89–93.
17. Ling, K., R. L. Doughman, V. V. Iyer, A. J. Firestone, S. F. Bairstow, D. F. Mosher, M. D. Schaller, and R. A. Anderson. 2003. Tyrosine phosphorylation of type I$\gamma$ phosphatidylinositol phosphate kinase by Src regulates an integrin-talin switch. *J. Cell Biol.* 163: 1339–1349.
18. Di Paolo, G., L. Pellegrini, K. Letinic, G. Cestra, R. Zoncu, S. Voronov, S. Chang, J. Guo, M. R. Wenk, and P. De Camilli. 2002. Recruitment and regulation of phosphatidylinositol phosphate kinase type 1$\gamma$ by the FERM domain of talin. *Nature* 420: 85–89.
19. Tremuth, L., S. Kreis, C. Melchior, J. Hoebeke, P. Ronde, S. Plancon, K. Takeda, and N. Kieffer. 2004. A fluorescence cell biology approach to map the second integrin-binding site of talin to a 130-amino acid sequence within the rod domain. *J. Biol. Chem.* 279: 22258–22266.
20. Bass, M. D., B. J. Smith, S. A. Prigent, and D. R. Critchley. 1999. Talin contains three similar vinculin-binding sites predicted to form an amphipathic helix. *Biochem. J.* 341: 257–263.
21. Jockusch, B. M., and M. Rudiger. 1996. Crosstalk between cell adhesion molecules: vinculin as a paradigm for regulation by conformation. *Trends Cell Biol.* 6: 311–315.
22. Kim, M., C. V. Carman, and T. A. Springer. 2003. Bidirectional transmembrane signaling by cytoplasmic domain separation in integrins. *Science* 301: 1720–1725.
23. Tadokoro, S., S. J. Shattil, K. Eto, V. Tai, R. C. Liddington, J. M. de Pereda, M. H. Ginsberg, and D. A. Calderwood. 2003. Talin binding to integrin $\beta$ tails: a final common step in integrin activation. *Science* 302: 103–106.
24. Martel, V., C. Racaud-Sultan, S. Dupe, C. Marie, F. Paulhe, A. Galmiche, M. R. Block, and C. Albiges-Rizo. 2001. Conformation, localization, and integrin binding of talin depend on its interaction with phosphoinositides. *J. Biol. Chem.* 276: 21217–21227.
25. Nieswandt, B., M. Moser, I. Pleines, D. Varga-Szabo, S. Monkley, D. Critchley, and R. Fassler. 2007. Loss of talin1 in platelets abrogates integrin activation, platelet aggregation, and thrombus formation in vitro and in vivo. *J. Exp. Med.* 204: 3113–3118.
26. Vyas, Y. M., K. M. Mehta, M. Morgan, H. Maniar, L. Butros, S. Jung, J. K. Burkhardt, and B. Dupont. 2001. Spatial organization of signal transduction molecules in the NK cell immune synapses during MHC class I-regulated noncytolytic and cytolytic interactions. *J. Immunol.* 167: 4358–4367.
27. Kuhn, J. R., and M. Poenie. 2002. Dynamic polarization of the microtubule cytoskeleton during CTL-mediated killing. *Immunity* 16: 111–121.
28. Priddle, H., L. Hemmings, S. Monkley, A. Woods, B. Patel, D. Sutton, G. A. Dunn, D. Zicha, and D. R. Critchley. 1998. Disruption of the talin gene compromises focal adhesion assembly in undifferentiated but not differentiated embryonic stem cells. *J. Cell Biol.* 142: 1121–1133.
29. Marwali, M. R., M. A. MacLeod, D. N. Muzia, and F. Takei. 2004. Lipid rafts mediate association of LFA-1 and CD3 and formation of the immunological synapse of CTL. *J. Immunol.* 173: 2960–2967.
30. Unkeless, J. C. 1979. Characterization of a monoclonal antibody directed against mouse macrophage and lymphocyte Fc receptors. *J. Exp. Med.* 150: 580–596.
31. Welder, C. A., D. H. Lee, and F. Takei. 1993. Inhibition of cell adhesion by microspheres coated with recombinant soluble intercellular adhesion molecule-1. *J. Immunol.* 150: 2203–2210.
32. Lian, R. H., M. Maeda, S. Lohwasser, M. Delcommenne, T. Nakano, R. E. Vance, D. H. Raulet, and F. Takei. 2002. Orderly and nonstochastic acquisition of CD94/NKG2 receptors by developing NK cells derived from embryonic stem cells in vitro. *J. Immunol.* 168: 4980–4987.
33. Tabatabaei-Zavareh, N., A. Vlasova, C. P. Greenwood, and F. Takei. 2007. Characterization of developmental pathway of natural killer cells from embryonic stem cells in vitro. *PLoS One* 2: e232.
34. Maeda, M., C. Carpenito, R. C. Russell, J. Dasanjh, L. L. Veinotte, H. Ohta, T. Yamamura, R. Tan, and F. Takei. 2005. Murine CD160, Ig-like receptor on NK cells and NKT cells, recognizes classical and nonclassical MHC class I and regulates NK cell activation. *J. Immunol.* 175: 4426–4432.
35. Ebeling, O., A. Duczmal, S. Aigner, C. Geiger, S. Schollhammer, J. T. Kemshead, P. Moller, R. Schwartz-Albiez, and P. Altevogt. 1996. L1 adhesion molecule on human lymphocytes and monocytes: expression and involvement in binding to $\alpha_v\beta_3$ integrin. *Eur. J. Immunol.* 26: 2508–2516.
36. Monkley, S. J., X. H. Zhou, S. J. Kinston, S. M. Giblett, L. Hemmings, H. Priddle, J. E. Brown, C. A. Pritchard, D. R. Critchley, and R. Fassler. 2000. Disruption of the talin gene arrests mouse development at the gastrulation stage. *Dev. Dyn.* 219: 560–574.
37. Monkley, S. J., C. A. Pritchard, and D. R. Critchley. 2001. Analysis of the mammalian talin2 gene TLN2. *Biochem. Biophys. Res. Commun.* 286: 880–885.
38. Gailit, J., and E. Ruoslahti. 1988. Regulation of the fibronectin receptor affinity by divalent cations. *J. Biol. Chem.* 263: 12927–12932.
39. Shimizu, Y., and J. L. Mobley. 1993. Distinct divalent cation requirements for integrin-mediated $CD4^+$ T lymphocyte adhesion to ICAM-1, fibronectin, VCAM-1, and invasin. *J. Immunol.* 151: 4106–4115.
40. Rodriguez-Fernandez, J. L., M. Gomez, A. Luque, N. Hogg, F. Sanchez-Madrid, and C. Cabanas. 1999. The interaction of activated integrin lymphocyte function-associated antigen 1 with ligand intercellular adhesion molecule 1 induces activation and redistribution of focal adhesion kinase and proline-rich tyrosine kinase 2 in T lymphocytes. *Mol. Biol. Cell* 10: 1891–1907.
41. Koziak, K., E. Kaczmarek, S. Y. Park, Y. Fu, S. Avraham, and H. Avraham. 2001. RAFTK/Pyk2 involvement in platelet activation is mediated by phosphoinositide 3-kinase. *Br. J. Haematol.* 114: 134–140.
42. McShan, G. D., R. Zagozdzon, S. Y. Park, S. Zrihan-Licht, Y. Fu, S. Avraham, and H. Avraham. 2002. Csk homologous kinase associates with RAFTK/Pyk2 in breast cancer cells and negatively regulates its activation and breast cancer cell migration. *Int. J. Oncol.* 21: 197–205.
43. Simonson, W. T., S. J. Franco, and A. Huttenlocher. 2006. Talin1 regulates TCR-mediated LFA-1 function. *J. Immunol.* 177: 7707–7714.
44. Cluzel, C., F. Saltel, J. Lussi, F. Paulhe, B. A. Imhof, and B. Wehrle-Haller. 2005. The mechanisms and dynamics of $\alpha_v\beta_3$ integrin clustering in living cells. *J. Cell Biol.* 171: 383–392.
45. Tanentzapf, G., and N. H. Brown. 2006. An interaction between integrin and the talin FERM domain mediates integrin activation but not linkage to the cytoskeleton. *Nat. Cell Biol.* 8: 601–606.
46. Orange, J. S., N. Ramesh, E. Remold-O'Donnell, Y. Sasahara, L. Koopman, M. Byrne, F. A. Bonilla, F. S. Rosen, R. S. Geha, and J. L. Strominger. 2002. Wiskott-Aldrich syndrome protein is required for NK cell cytotoxicity and colocalizes with actin to NK cell-activating immunologic synapses. *Proc. Natl. Acad. Sci. USA* 99: 11351–11356.
47. Miletic, A. V., M. Swat, K. Fujikawa, and W. Swat. 2003. Cytoskeletal remodeling in lymphocyte activation. *Curr. Opin. Immunol.* 15: 261–268.
48. Turner, C. E., J. R. Glenney, Jr., and K. Burridge. 1990. Paxillin: a new vinculin-binding protein present in focal adhesions. *J. Cell Biol.* 111: 1059–1068.
49. McGregor, A., A. D. Blanchard, A. J. Rowe, and D. R. Critchley. 1994. Identification of the vinculin-binding site in the cytoskeletal protein $\alpha$-actinin. *Biochem. J.* 301: 225–233.
50. Tsukita, S., K. Oishi, N. Sato, J. Sagara, A. Kawai, and S. Tsukita. 1994. ERM family members as molecular linkers between the cell surface glycoprotein CD44 and actin-based cytoskeletons. *J. Cell Biol.* 126: 391–401.